The steering control of an experimental autonomous vehicle

by N.E. Pears, BSc, PhD and J.R. Bumby, BSc, PhD, CEng, MIEE

Experimental results relating to the steering control system of an experimental autonomous vehicle operating in a pre-defined and structured environment are presented. A method of steering control is formulated which relates second-order criteria, such as rise time and damping factor, to the parameters of the control system. With the control system described, the vehicle can track a path of constant heading with very little steady-state error and, if the control parameters are chosen in the correct ratio, it will respond in a critically damped fashion to the step disturbances which are generated by position corrections. For a curved path, demand curvature is treated as an input to the system in order to eliminate steady-state offset errors in tracking. In order to make the vehicle's performance independent of velocity, control parameters are derived as simple functions of velocity. This has the effect of allowing the vehicle to manoeuvre more tightly at lower speeds, and makes use of the increased availability of drive-system torque at such speeds. In order to prevent stalling of the stepper-motor drive system at large changes in demand curvature, a method of limiting the rate of steering is described.

Keywords: Autonomous guided vehicles, AGV control, AGV dynamics

List of Symbols

Symbol		*Units*
G_{cl}	Closed-loop transfer function of the control system	
G_{ol}	Open-loop transfer function of the control system	
G_{lb}	Transfer function of the limiting block	
k_1	Curvature-rate limiting constant	
$k_{\theta'}$	Local angle (θ') proportional control constant	
k_y	Local distance (y) proportional control constant	
r	Radius described by the AGV's reference point	(m)
r_{seg}	Radius of a curved command segment	(m)
t_r	Rise time	(s)
T_s	Sampling interval	(s)
V	Base velocity: velocity of the AGV's reference point	(m/s)
x, y, θ'	Coordinates in a path-dependent local reference frame	
X, Y, θ	Coordinates in a global reference frame	
y	Perpendicular distance to path in a local frame	(m)
y_{lw}	Separation of demand path and correction board	(m)
Y_{lw}, Y	Laplace-transformed value of y_{lw} and y, respectively	
y_{ss}	Steady-state value of perpendicular distance error	(m)
κ	Actual vehicle turning curvature	(m^{-1})
κ_{dem}	Demand (unlimited) AGV turning curvature	(m^{-1})
κ_{lp}	Demand curvature derived from local position	(m^{-1})
κ_{seg}	Curvature of current command path	(m^{-1})
κ_{ss}	Steady-state value of turning curvature	(m^{-1})
θ	Heading in a global frame	(rad)
θ'	Heading in a path-dependent local reference frame	(rad)
θ'_r	Demand heading relative to demand path	(rad)
θ'_{ss}	Steady-state value of local angle	(rad)
ξ	Damping factor	
ω_n	Undamped natural frequency	(rad/s)

Subscripts

i	Index of ith control interval	
ss	Subscript denoting steady state	
t	Time	(s)

School of Engineering and Applied Science, University of Durham, South Road, Durham, England DH1 3LE

1. Introduction

Traditionally, autonomous guided vehicles (AGVs) have been guided around their environment by wires buried under the floor of a warehouse or factory. The AGV follows the wires by monitoring the difference in induced voltage between two coils on the vehicle and uses this information to generate steering instructions (Anon, 1985a, 1985b). Although this type of guidance system is simple, proven, and reliable, a good deal of flexibility is lost as the choice of vehicle routing is dictated by the layout of the wires. In this paper a 'free-ranging' guidance method is described which uses ultrasonic sensing and odometry in a complementary fashion. This guidance method requires that a number of corrections boards, tailored to the operation of the ultrasonic sensors be placed within the vehicle's workspace (Pears, 1989). Obviously, the use of a minimal set of sensors cannot provide the vehicle with a high degree of autonomy; rather, the aim is to develop data processing and control techniques that constitute a method of low-level guidance that does not limit the speed or efficiency of the vehicle's movements. This paper focuses upon the steering-control system that constitutes part of that guidance method.

In the last 20 years or so substantial research effort has been directed towards the development of mobile robots in order to study various aspects of AGV performance, behaviour and control. Some of the more notable experimental autonomous vehicles include SHAKEY (Nilsson, 1969), HILARE (Giralt *et al*, 1979), the CMU ROVER (Elfes and Talukdar, 1983), the GSR (Harmon, 1987), the TERRAGATOR (Kande *et al*, 1985) and the IMP (Crowley, 1985) (a comprehensive reference of AGV research is given in the bibliography of Warwick and Brady (1986)). More recently, ideas concerning redundant multisensors (Durrant-Whyte, 1987), mobile robot architectures (Brooks, 1986), world modelling (Elfes, 1986) and obstacle avoidance, (Krough, 1984) have been researched. Of particular relevance to this paper is that work typical of the research aimed at vehicle guidance along a prescribed path. For example, automated passenger vehicles in which conventional four-wheeled front-steered cars have been made to follow a guide-wire have been reported (Fenton *et al*, 1976; Cormier and Fenton, 1980). Stephens *et al* (1983) described a scheme whereby incremental reference vectors are moved at demand speed through a defined trajectory to form a kind of 'tow-along' procedure. Steer (1985) investigated wall-following using a single ultrasonic sensor on the front corner of a vehicle with front-wheel steering. In this work, a simple model was examined in which curvature was made to be proportional to the difference in measured distance and a demand distance. Kim (1987) has presented a theoretical optimal (and suboptimal) proportional-plus-integral controller for a wire-guidance vehicle. Hongo *et al* (1987) have described a control method whereby the accelerations of the left and right drive wheels are controlled such that the vehicle's state (position, orientation, and velocity) will agree with that of the current command

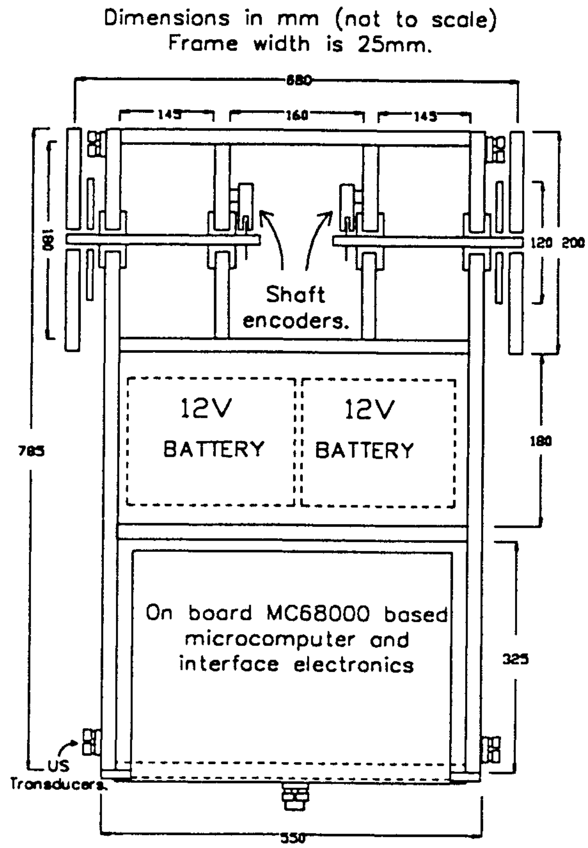

Fig 1a Plan view of the research AGV

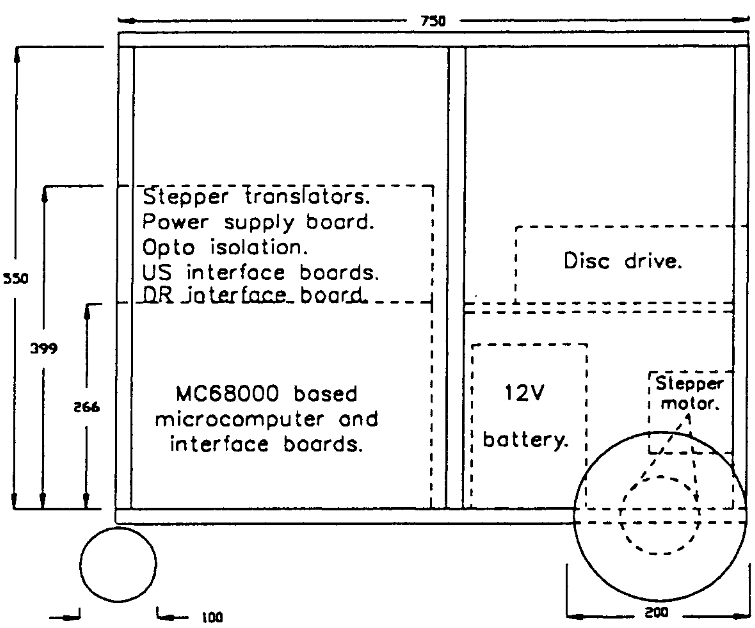

Fig 1b Side view of the research AGV

after a given time period. In this work, accelerations were used as the controlling variables to avoid sudden changes in velocity. In comparison with most of these systems, the steering control described here is simple on account of the nature of the vehicle's drive system and the effectiveness of the basic control rule.

In the following sections, the results of experimental tests on a steering control system for an autonomous guided vehicle are presented and compared with theoretical predicted behaviour. Sections 2 and 3 describe briefly the structure of the experimental vehicle and the control law that is used in its control. Section 4 then presents a simple analysis to predict the vehicle's behaviour to small disturbances. This analysis allows the vehicle's behaviour to be related to second-order criteria such as damping factor and rise time and is used to explain the experimental results of Sections 5 and 6. Finally, the analysis is expanded to include the effect of limiting the rate of steering within the control system.

2. The experimental vehicle

To conduct the experimental work, an autonomous vehicle has been designed and built [full details are given in Pears and Bumby, 1990]. This vehicle, shown schematically in Fig 1, has two rear drive wheels each independently driven by separate stepper motors. Steering is implemented by controlling the speed differential between these two drive wheels. Optical shaft encoders are used to generate odometric information and are mounted on each drive wheel, while five sets of ultrasonic transducers are mounted around the perimeter of the vehicle; those at each corner provide position–correction information, while that at the front of the vehicle is used to sense obstacles. All the vehicle control is implemented on a Motorola 68000 microprocessor system.

3. Formulation of a control law

Fundamental to the steering control is the decision as to what positional information should be used in the steering control loop and how it should be used. The control problem itself if multi-variable in that both yaw angle and perpendicular distance relative to the demand path must be controlled.

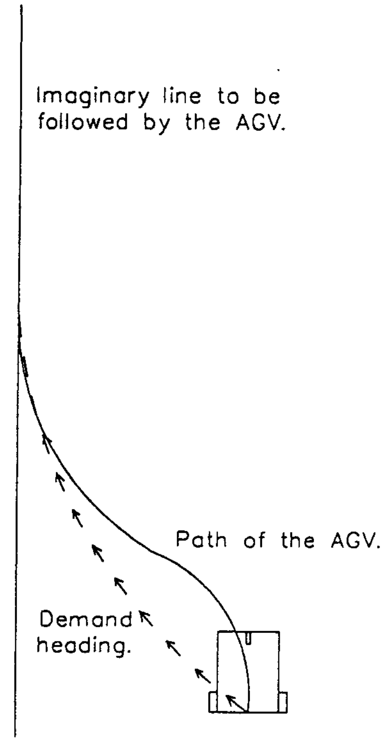

Fig 2 The control method

Since the heading of the AGV affects the way in which distance error changes, the control algorithm must initially generate a demand heading relative to the heading of the required path. This demand heading always points towards the demand path on a gradient that is proportional to the distance error. The error in AGV heading, with respect to a demand heading, can then be used to yield a turning curvature (through a proportional controller) that tends to diminish this heading error. In effect, the AGV can turn left and then right by steering around each of the small heading lines shown in Fig 2.

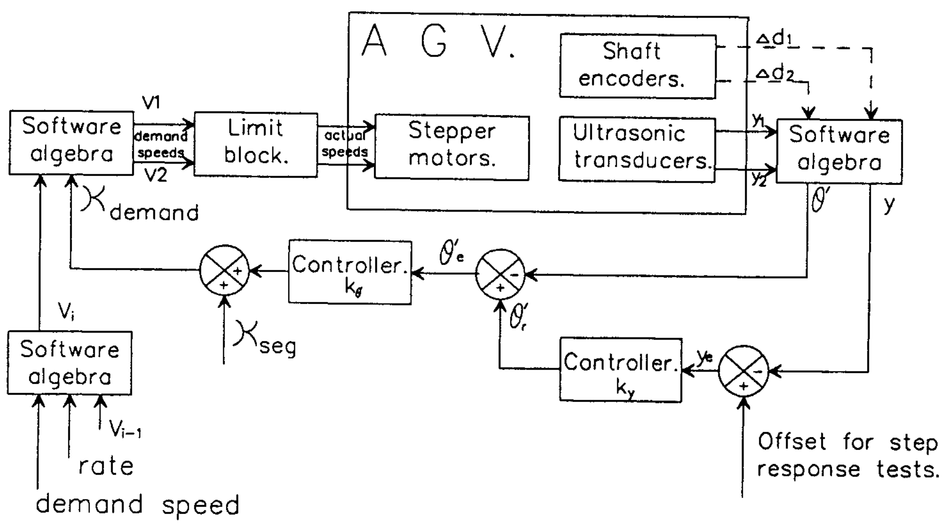

Fig 3 Block diagram of the control system

4. Analysis of the basic steering-control system

A knowledge of the steady-state performance of the steering control system is required to determine how close the vehicle stays to its designed course as it moves through the environment. Since position corrections periodically subject the vehicle to step changes in apparent perpendicular distance and orientation relative to its demand path, a knowledge of the system's response to step disturbances is also required.

The initial control system configuration is shown in Fig 3. A complete analysis of this system for a conventionally steered vehicle requires consideration of the interaction between the vehicle dynamics, kinematics and the control law. However, since stepper motors are used to drive the AGV, the vehicle dynamics reduce to a simple unity-gain function. The reason for this is that the speed of each wheel is always directly proportional to the speed input to the stepper-motor driver (if this were not the case then the stepper drive would have lost steps and stalled). In addition, the speed of response of the motor is directly proportional to the rate at which the velocity input demand changes. In the control system, small changes in input demand may be instantaneous, while for larger changes the rate of change of velocity demand will be limited to prevent the stepper motor from stalling. The analysis now presented represents the vehicle and motor dynamics as a unity-gain function, although an extension to this work in Section 7 includes the necessary transfer function to represent the limits imposed on the rate of change of velocity demand to each drive wheel. If other types of drive motor were used, then the speed of response of each motor would be dependent on AGV and motor-inertia effects and should be considered in detail.

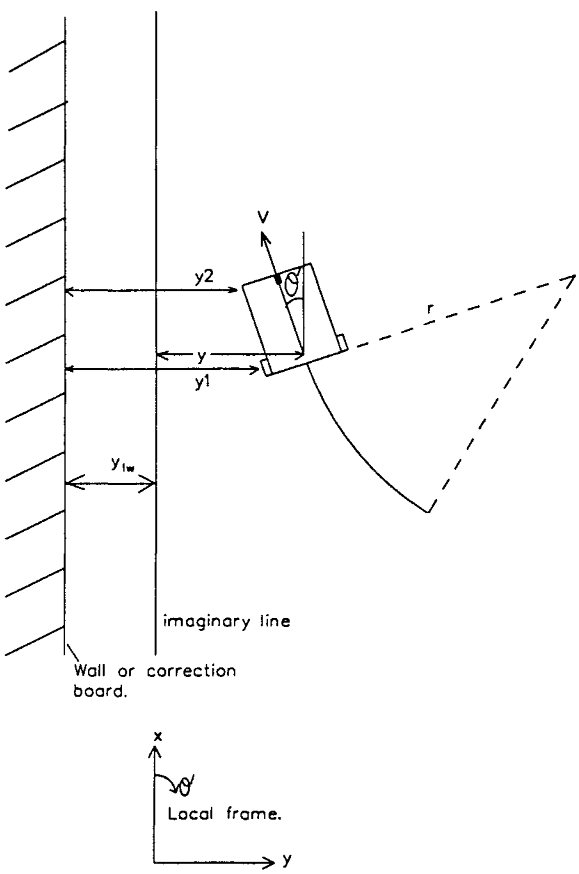

Fig 4 The line-following process

Using Fig 3 and the AGV information defined in Fig 4, the basic control equations can be written as

$$\theta'_r = -k_y(y - y_{lw}) \qquad \ldots(1)$$

$$\kappa = k_{\theta'}(\theta'_r - \theta') \qquad \ldots(2)$$

where k_y and $k_{\theta'}$ are simple proportional controller gains.

Combining Eqns (1) and (2) gives

$$\kappa = -k_{\theta'}k_y y - k_{\theta'}\theta' + k_{\theta'}k_y y_{lw} \qquad \ldots(3)$$

showing that if two of the three quantities y, θ', and κ, are known, then the third can be derived. Consequently, any pair of variables is independent and can be chosen to represent the system. In this instance the system states are arbitrarily chosen as y and θ' with the system input being y_{lw}.

For a vehicle moving towards its demand path as shown in Fig 4, the rate of change of perpendicular distance, y, in the local coordinate frame of the command is given by

$$\dot{y} = V\sin\theta' \qquad \ldots(4)$$

and if θ' is sufficiently small:

$$\dot{y} \approx V\theta' \qquad \ldots(5)$$

[In the experiment described in the following section, the vehicle was subjected to a step change in y of 20 cm and the largest angle (θ') attained by the AGV was 8.5 degrees. In this case the maximum error incurred by the above approximation is less than 1%.]

Note also that

$$\dot{\theta}' = V\kappa \qquad \ldots(6)$$

when

$$\begin{bmatrix} \dot{y} \\ \dot{\theta}' \end{bmatrix} = \begin{bmatrix} 0 & V \\ -k_{\theta'}k_y V & -k_{\theta'}V \end{bmatrix} \begin{bmatrix} y \\ \theta' \end{bmatrix} + \begin{bmatrix} 0 \\ k_{\theta'}k_y V \end{bmatrix} [y_{lw}] \qquad \ldots(7)$$

The closed-loop transfer function, $G_{cl}(s)$, and the open-loop transfer function $G_{ol}(s)$, can be derived from Eqn (7) as

$$G_{cl}(s) = \frac{Y(s)}{Y_{lw}(s)} = \frac{k_{\theta'}k_y V^2}{s^2 + k_{\theta'}Vs + k_{\theta'}k_y V^2} \qquad \ldots(8)$$

and

$$G_{ol}(s) = \frac{G_{cl}(s)}{1 - G_{cl}(s)} = \frac{k_y k_{\theta'}V^2}{s(s + k_{\theta'}V)} \qquad \ldots(9)$$

with the position of the closed-loop poles being given by

$$s_{1,2} = -\frac{k_{\theta'}V}{2} \pm \frac{V}{2}\sqrt{k_{\theta'}^2 - 4k_{\theta'}k_y} \qquad \ldots(10)$$

When $k_{\theta'} = 4k_y$, critical damping is obtained and the AGV's position is given by the standard equation

$$y = 1 - e^{-\omega_n t}(1 + \omega_n t) \qquad \ldots(11)$$

If $k_{\theta'} < 4k_y$ then the AGV's motion will be underdamped with a natural frequency of

$$\omega_n = V\sqrt{k_{\theta'} k_y} \qquad \ldots(12)$$

and damping factor

$$\xi = \frac{1}{2}\sqrt{\frac{k_{\theta'}}{k_y}} \qquad \ldots(13)$$

Eqn (10) shows that a critically damped vehicle response can be achieved by setting the controller gains $k_{\theta'}$ and k_y such that

$$k_{\theta'} = 4k_y \qquad \ldots(14)$$

but that, not surprisingly, the rise time of vehicle motion is velocity-dependent. This velocity dependency can be removed by setting

$$k_{\theta'} = k/V \qquad \ldots(15a)$$

$$k_y = k_{\theta'}/4 \qquad \ldots(15b)$$

when the position of the closed-loop poles will be independent of velocity; the value of k being selected to obtain the desired rise time.

5. Performance of the control system in line following

To test the accuracy of the theory outlined in Section 4, the experimental AGV was allowed to reach a speed of 0.2 m/s before being subjected to a 20 cm step change in position, ie, a step change in $y_{l/w}$. Experiments were conducted using uncorrected odometric measurements, derived from the internal shaft encoders, as feedback. (If position corrections had been permitted during the experiment, it would have been difficult to assess the performance of the control system, as corrections would have acted as additional step disturbances.) In this experiment the curvature-rate limit block was removed from the control loop.

The first graph, Fig 5a, shows the path of the vehicle, while Fig 5b indicates how the distance error (ie, the distance between the midpoint of the AGV's drive wheels and the vehicle's demand path) varies with time when the control constants are chosen to give critical damping ($k_{\theta'} = 4$, $k_y = 1$). From Fig 5b it can be seen that distance error is reduced to under 5% of the initial error (ie, within 1 cm) approximately 12 s after the step change was introduced. This should be compared with the 11.9 s predicted by Eqn (11). As shown in Fig 5c, the AGV reaches headings of up to 8.5° relative to the line during this test while the large initial change in curvature (0.8 m^{-1}) that the step change generates is apparent in Fig 5d. Fig 5d further indicates that the vehicle turned right (positive curvature) and then left (negative curvature) with curvature reducing gradually as it approached its designed course.

Fig 6 shows the path of the AGV when the control constants are chosen to give underdamping ($k_{\theta'} = 1$, $k_y = 3$). The damping factor calculated using these constants is 0.289 which corresponds to an overshoot of 39% and compares well with the measured overshoot of 40%.

The relationship between the control constants can

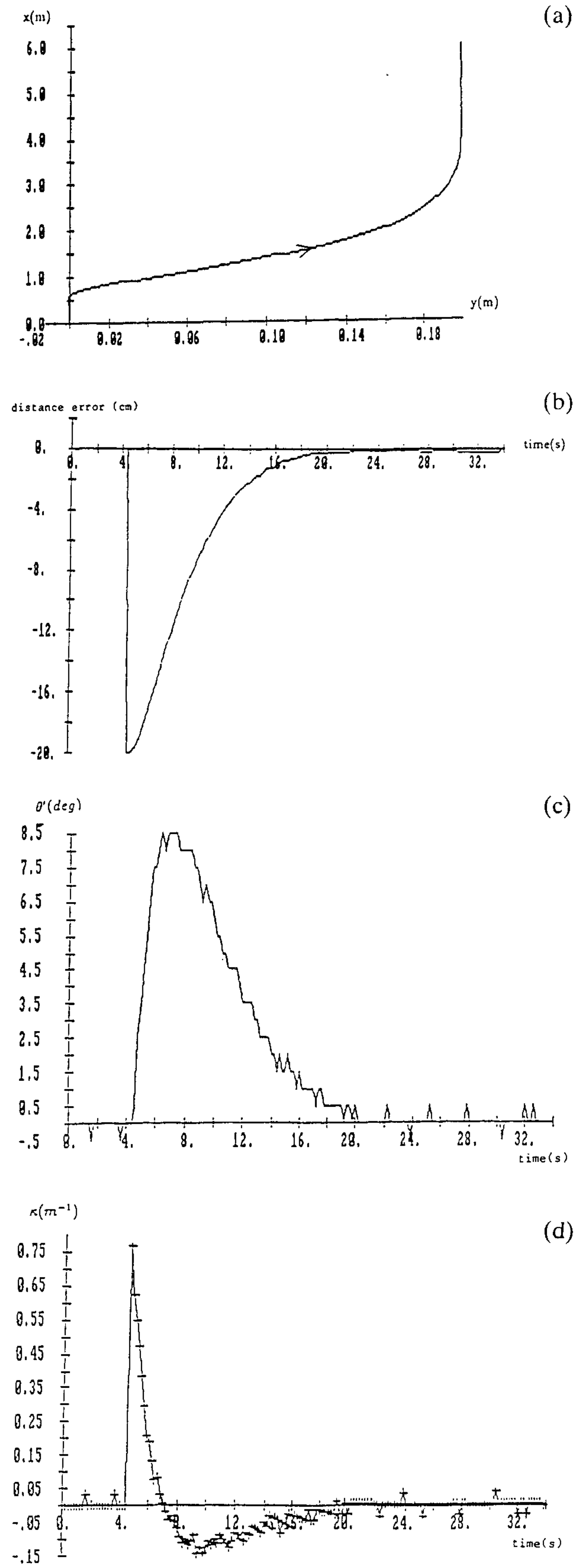

Fig 5 Critically damped response $k_{\theta'} = 4$, $k_y = 1$, $V = 0.2$ m/s: (a) AGV path in step-response test; (b) Distance error against time; (c) Local angle, θ', against time; (d) Curvature, κ, against time

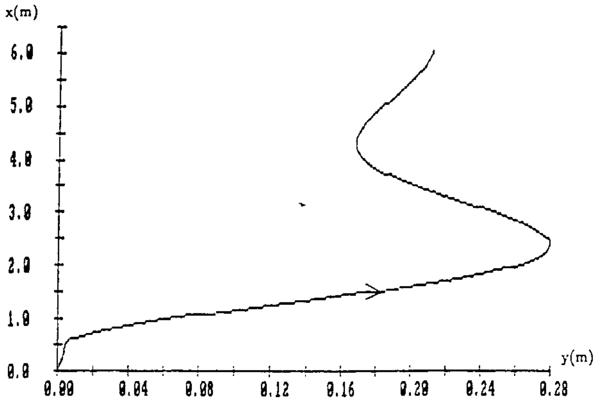

Fig 6 Path of AGV with underdamped response. Step response: $k_{\theta'} = 1$, $k_y = 3$, $V = 0.2$ m/s

be explained qualitatively. If k_y is large, the vehicle's demand heading relative to the new demand path (ie, relative to the parallel 20 cm offset) is steep and only at very small distance errors will the demand heading decay to zero. Since $k_{\theta'}$ is small, only relatively small curvatures are generated and the AGV cannot attain the large changes in demand heading set by k_y. This lag, generated because $k_{\theta'}$ is small compared to k_y, causes the vehicle to cross its new demand path, and oscillations will ensue until demand headings are small enough to be attained by the value of $k_{\theta'}$.

Given that the control constants are chosen in the correct ratio to give critical damping, the rise time of the AGV's motion is dependent on the value $1/V\sqrt{k_{\theta'}k_y}$. This dependency of the rise time on vehicle velocity can be removed by making $k_{\theta'}$ and k_y velocity-dependent as explained by Eqn (15). Thus for a velocity of 0.2 m/s, control constants of $k_{\theta'} = 4$ and $k_y = 1$ are employed, whereas if the vehicle were travelling slower, at 0.1 m/s, then, in order to obtain the same response time as in Fig 5, a higher gain would be necessary, in this case $k_{\theta'} = 8$, $k_y = 2$ ($k = 1.25$ in Eqn (15a)). These velocity-dependent control parameters cause the vehicle to approach its path more steeply, since k_y is higher, when travelling more slowly. This is a sensible approach since, for a given rate of change of curvature, smaller angular accelerations are developed at a lower base velocity ($\theta' = V\kappa$). With this scheme, the torque demand on the stepper motors increases in inverse proportion to velocity, since each time velocity is reduced by half, both $k_{\theta'}$ and k_y are doubled. Thus, the initial demand rate of change of curvature after a step disturbance is multiplied fourfold, and both the initial angular acceleration and demand torque are doubled. As a consequence of this, the control method is particularly suited to a stepper-motor drive, which can provide much larger torques at low stepping rates.

This constant rise time feature of the control system becomes particularly important as the vehicle approaches its destination because, if a position correction occurs just before the goal position is reached, a poor rise time may not allow the vehicle to reach its goal position with good accuracy (ie, some control error may still exist at the goal position). The use of velocity-dependent control parameters means that the forward travelling distance required to attain 95% of a lateral position correction is proportional to

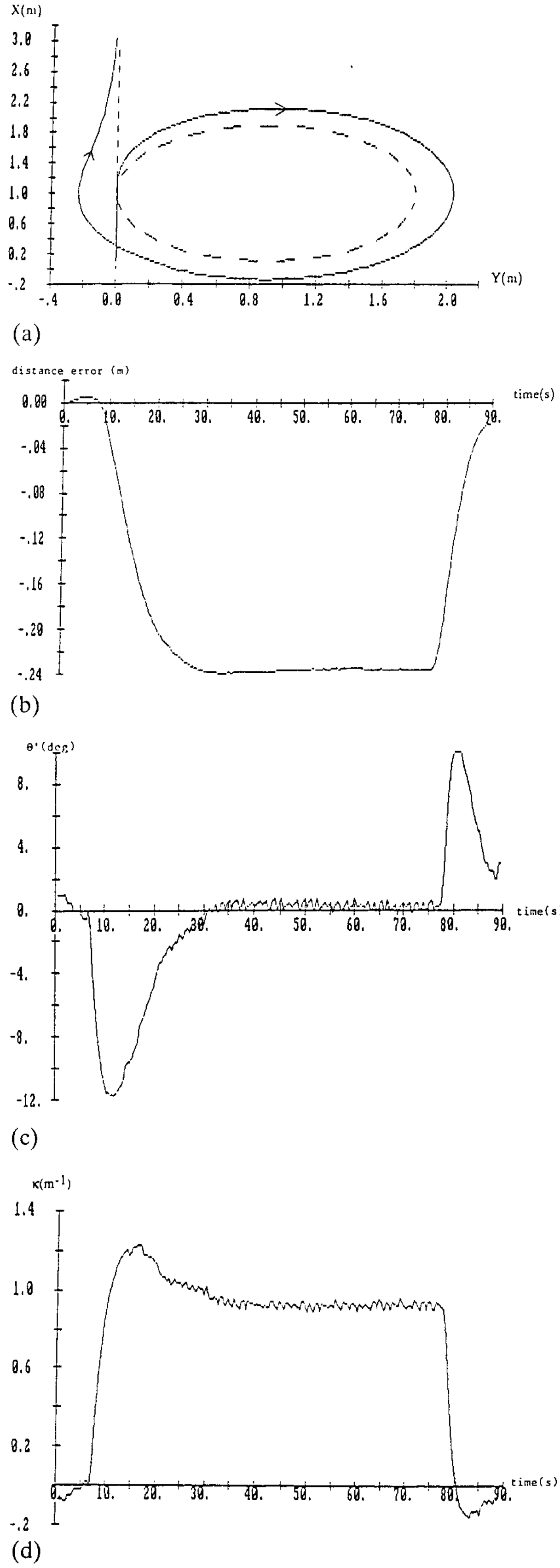

Fig 7 Curve-tracking test $k_{\theta'} = 4$, $k_y = 1$, $V = 0.1$ m/s (a) AGV path in a curve-tracking test; (b) Distance error against time; (c) Local angle, θ', against time; (d) Curvature, κ, against time

velocity. Constancy of rise time ensures a good control accuracy at the vehicle's destination and can be compared to the common experience of severely reducing speed, while parking a car, in order to steer more sharply.

It is obvious from Eqn (15) that at low base velocities, large control constants are generated. A large value of k_y suggests that the vehicle's approach to its demand path is steep. Such an approach invalidates the small angle approximation made in Eqn (5) and the vehicle's behaviour would deviate from that predicted. To prevent this happening if the base velocity is below 0.1 m/s, the control constants are held at $k_{\theta'} = 8$ and $k_y = 2$, with a consequent reduction in rise time at low speeds.

6. Performance of the control system in tracking a curve

In order to determine how well the control system performs when tracking a curve, the AGV was asked to accelerate to 0.2 m/s on a heading of 0.0 degrees to a position, $X, Y = (1.0, 0.0)$. The AGV then executes a full (360°) circle on a radius of 0.9 m, and finally follows a straight path to the position $X, Y = (3.0, 0.0)$. Fig 7a shows the path of the vehicle where it is apparent that a large steady-state offset develops quickly. This steady-state offset is clearly shown in Fig 7b and indicates that the disturbance caused by the path curvature precipitates a steady-state error in the state y of approximately -23 cm. Rearranging Eqn (3), and using the subscript '*ss*' to denote steady-state values, the steady-state value of the local perpendicular distance to the demand path is given by:

$$y_{ss} = -\frac{1}{k_{\theta'} k_y}(\kappa_{ss} + k_{\theta'} \theta'_{ss}) \qquad \ldots(16)$$

In the steady state the vehicle must be travelling parallel to, if not on, its demand path, as can be seen in Fig 7a. This implies that the steady-state value of local angle error, θ'_{ss}, must be near to zero. Fig 7c shows the changes in local angle at entry and exit of the curve follow command and verifies this.

The steady-state error in y can be used to form the steady-state curvature as

$$\kappa_{ss} = \frac{1}{r_{seg} - y_{ss}} \qquad \ldots(17)$$

where r_{seg} is the radius of the required path. Setting $\theta'_{ss} = 0$, substituting Eqn (17) into Eqn (16) and rearranging gives:

$$y_{ss} = \frac{r_{seg} \pm \sqrt{r_{seg}^2 + \dfrac{4}{k_{\psi'} k_y}}}{2} \qquad \ldots(18)$$

Eqn (18) shows that the steady-state offset, y_{ss}, is dependent on the path curvature ($\kappa_{seg} = 1/r_{seg}$) and the choice of control constants. Substituting values of $r_{seg} = 0.9$, $k_{\theta'} = 4$, and $k_y = 1$ gives $y_{ss} = -22.27$ cm, which is in close agreement with the value obtained from Fig 7b. The steady-state curvature, given by Eqn (17) is 0.89 m^{-1} which is consistent with Fig 7d.

Since a non-zero value of y_{ss} must exist in order to generate the curvature of a path parallel to that of the command segment, the use of proportional controllers and local position information (y, θ') only is inadequate for tracking a curve. Although the inclusion of an integrating term in addition to k_y could reduce steady-state errors in curve tracking, it is preferable to consider the path curvature as an input to the control system.

The curvature of the demand path modifies the rate of change of local yaw angle, Eqn (6), as

$$\dot{\theta}' = V(\kappa - \kappa_{seg}) \qquad \ldots(19)$$

where κ_{seg} is the curvature of the path. This path

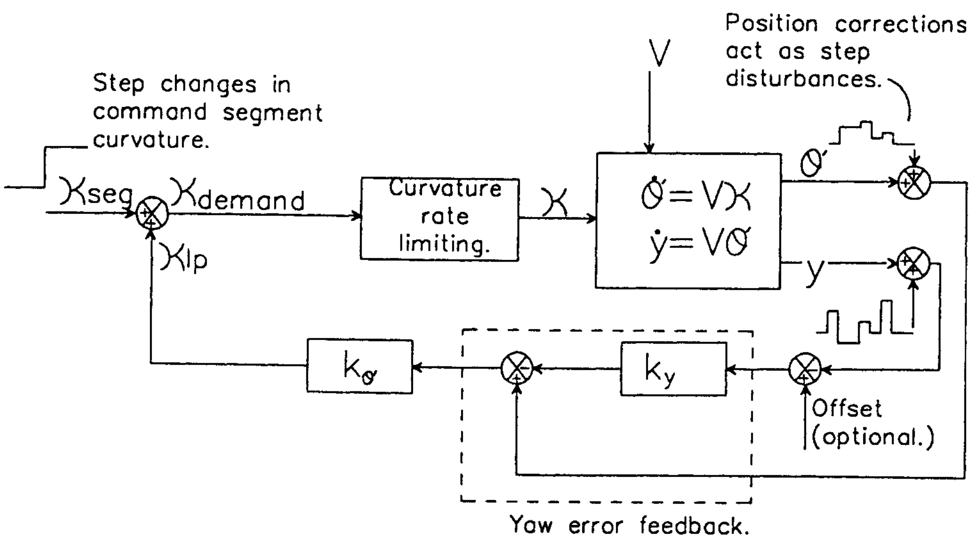

$$\theta'_e = \begin{bmatrix} -k_y, & 1 \end{bmatrix} \begin{bmatrix} y \\ \theta' \end{bmatrix}$$

Fig 8 The modified control system

curvature generates a demand yaw-angle rate such that the state equation (Eqn (7)) is modified to

$$\begin{bmatrix} \dot{y} \\ \dot{\theta}' \end{bmatrix} = \begin{bmatrix} 0 & V \\ -k_{\theta'} k_y V & -k_{\theta'} V \end{bmatrix} \begin{bmatrix} y \\ \theta' \end{bmatrix} + \begin{bmatrix} 0 \\ V k_{\theta'} k_y \end{bmatrix} \begin{bmatrix} y_{lw} - \dfrac{\kappa_{seg}}{k_{\theta'} k_y} \end{bmatrix} \qquad \ldots(20)$$

If κ_{seg} is considered as an input, then this curvature is added to that derived from the measured local position (y, θ') before the required differential wheel speed is calculated. This is shown in the overview of the control system in Fig 8. Since specific path segments have specific constant path curvatures, a transition between one segment and the next applies a step input to the control system. Also shown in Fig 8 are position corrections acting as step disturbances on the states y and θ'. In this modified system, the curvature that is applied to the vehicle's drive wheels is redefined as the difference between the curvature derived from local position (y, θ') and the curvature of the demand path, rather than being derived from local position only. The state equation for curve following is now the same as that for line following, which is simply a special case, where $\kappa_{seg} = 0$.

More formally, if the curvature is redefined as

$$\kappa = \kappa_{lp} - \kappa_{seg} \qquad \ldots(21)$$

where

$$\kappa_{lp} = -k_{\theta'} [k_y, 1] \begin{bmatrix} y \\ \theta' \end{bmatrix} \qquad \ldots(22)$$

then the original state equation (Eqn (7)) describes the same performance in both line and curve following.

To test the accuracy of this modification to the control system, an experiment illustrated by Fig 9a was conducted with $k_{\theta'}$ and k_y set for critical damping. This shows the path of the AGV when it was asked to follow a line at a perpendicular displacement of 50 cm so that when it entered the subsequent curve-follow command, there was an initial error of 50 cm. This simulated an instance in which a large position correction occurs just before the vehicle enters a curve segment. Fig 9b shows that perpendicular distance error is reduced in a critically damped fashion, while tracking in the steady state gives almost zero error.

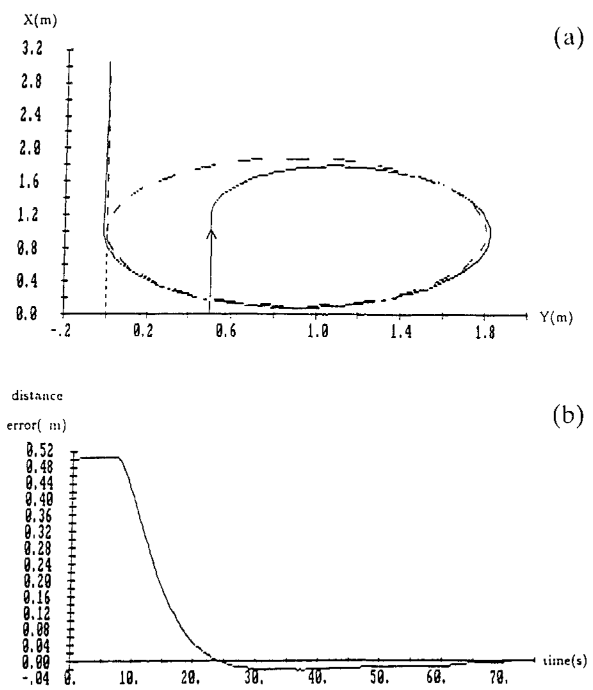

Fig 9 Curve-tracking performance with κ_{seg} input: (a) AGV path in curve-tracking system; (b) Distance error against time

7. Curvature-rate limiting

If the control constants ($k_{\theta'}$, k_y) are chosen to be high in order to give a short rise time, and the system is subjected to a large step change, the controller may generate a demand curvature high enough to stall the stepper motors. Section 4 explained how the control constants could be chosen according to velocity in order to give a rise time that was attainable for step disturbances of 20 cm or less. To make the control more robust, the rate of change of curvature (or rather the amount by which curvature can change at a control interval) is limited to prevent the stepper motors stalling in instances of position corrections of a greater magnitude.

The limiting method requires a limited curvature to be derived as a proportion of the difference between the current demand curvature (as derived from the vehicle's local position and the demand path curvature) and the curvature that was applied over the last control interval. Such a scheme was chosen because it is the simplest form of rate limiting, in which the steady-state value of the output eventually reaches that of a non-changing input and where the output is derived as a function of the input. The advantage of a limit block such as this is that its effect is predictable and can be included in the control analysis in order to maintain critical damping and a good, realistically attainable rise time.

The rate-limited curvature applied to the vehicle's drive wheels at control interrupt i is calculated as

$$\kappa_i = \kappa_{i-1} + k_1 (\kappa_{dem,i} - \kappa_{i-1}) \qquad \ldots(23)$$

where

$$\kappa_{dem,i} = \kappa_{lp,i} + \kappa_{seg} \qquad \ldots(24)$$

Eqn (23) has the form of a backward difference integration, in which the function integrated is the difference between the demand turning curvature and the curvature actually applied to the drive wheels and can be written in the form of a simple recursive digital filter as

$$G_{lb}(z) = \frac{\kappa_i}{\kappa_{dem,i}} = \frac{k_1 z}{z - (1 - k_1)} \qquad \ldots(25)$$

The backward difference mapping between the z and s domains gives

$$G_{lb}(s) = \frac{k_1}{k_1 + (1 - k_1) T_s s} = \frac{k'_1}{s + k'_1} \qquad \ldots(26)$$

where

$$k'_1 = \frac{k_1}{(1-k_1)\,T_s} \qquad \ldots(27)$$

If k_1 is set to one, $G_{lb}(s)$ is unity with Eqn (23), reducing to the unlimited case.

The introduction of the limiting block into the control loop modifies the system's open-loop transfer function (Eqn (9)) to:

$$G_{ol}(s) = \frac{k_{\theta'} k_y V^2 k'_1}{s(s+k_{\theta'} V)(s+k'_1)} \qquad \ldots(28)$$

The effect of the limit block is to introduce an additional pole on the real axis of the root locus at $-k'_1$. Again, $k_{\theta'}$ is generated in proportion to $1/V$ in order to fix one open-loop pole of the system, the choice of k_1 fixes another open-loop pole, and k_y is left to maintain critical damping of the closed-loop system.

Table 1 shows a number of results generated by a control design and analysis package in order to determine the best choice of k_1 and k_y. The columns in this table are the curvature-rate-limiting constant, the required k_y gain to maintain critical damping, the time to reach 95% of a step disturbance, and the magnitude of the step disturbance that is required to generate a demand change of curvature of $0.8\,\mathrm{m^{-1}}$ at the first control interrupt after the change (this is the approximate change in curvature at a control interval required to stall the drive system when travelling at a base velocity of 0.2 m/s). The results were generated with the assumption that $k_{\theta'} V = 0.8$.

Table 1 shows that although the system rise time improves as the degree of curvature-rate limiting is relaxed (ie, as k_1 increases), the step disturbance required to stall the drive system gradually approaches that of the unlimited system (20 cm). Since the magnitude of step disturbance cannot exceed the range of the vehicle's ultrasonic sensors (1.5 m), a value of 0.1 for k_1 provides a greater degree of limiting than is strictly necessary. A value of 0.2 for k_1 allows position corrections to be made that are compatible with the ultrasonic-measurement range. For a rise time of around 13.5 s and a velocity of 0.2 m/s, the vehicle is within 5% of its desired lateral position approximately 2.7 m after the step disturbance occurred. This has proved acceptable for the research rig. It is possible to improve the rise time of the system and yet maintain robustness with respect to step disturbances. This requires increasing $k_{\theta'}$ moving the pole $-k_{\theta'} V$ away from the imaginary axis while reducing k_1 moving the pole $-k'_1$ close to the imaginary axis.

Using the values

$$k_{\theta'} = 10,\ V = 0.2\,\mathrm{m/s},\ k_1 = 0.1,\ T_s = 0.1\,\mathrm{s}$$

TABLE 1: Predictions for curvature-rate-limited system

k_1	k_y	$t_r(s)$	$\frac{0.8}{k_{\theta'} k_y k_1}$ (m)
0.1	0.685	16.37	2.919
0.2	0.847	13.50	1.181
0.5	0.960	12.22	0.417
0.8	0.989	11.97	0.253
1.0	1.000	11.85	0.200

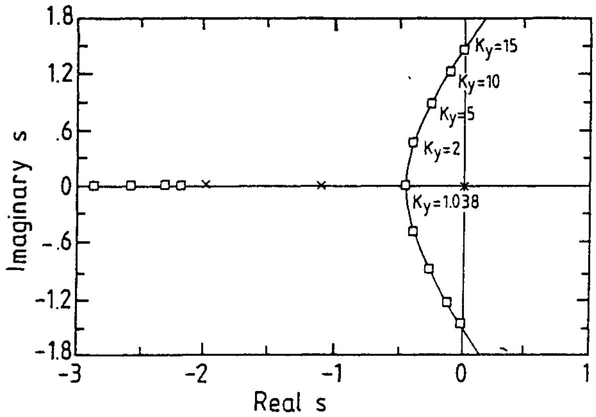

Fig 10 Root locus of curvature-limited system $k_{\theta'} = 10$, $k_l = 0.1$, $T_s = 0.1$ s, $V = 0.2$ m/s; × = open-loop poles; □ = closed-loop poles

the root-locus of Fig 10 is obtained. A k_y gain of 1.038 is required for critical damping, and the system becomes unstable at a gain of 15. With k_y set at the critically damped value, the simulation predicts a rise time of 10.85 s. Such a rise time is compatible with the non-curvature-rate-limited system (11.85 s), yet a step disturbance of 0.8 m is required to generate an immediate curvature change of $0.8\,\mathrm{m^{-1}}$. Fig 11a shows a

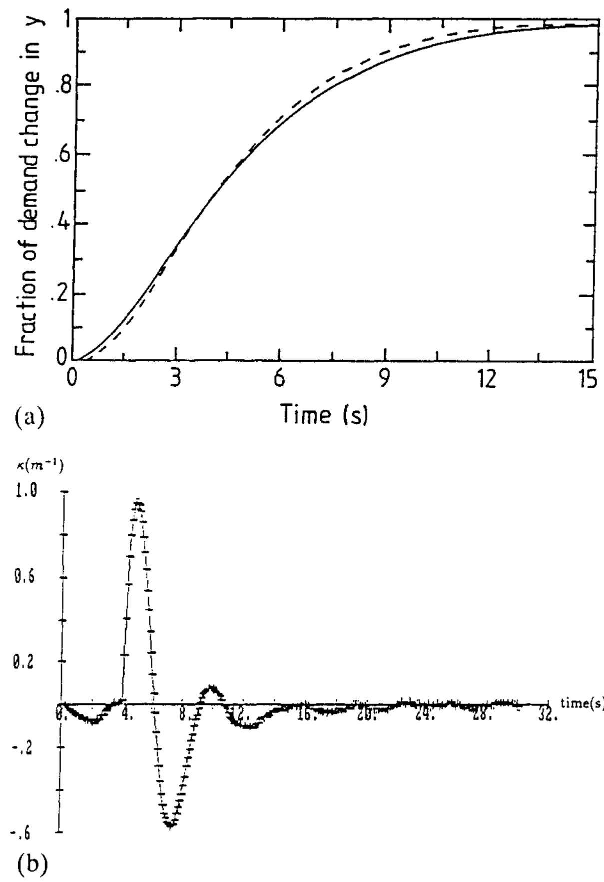

Fig 11 Showing the effect of curvature-rate limiting. (a) A comparison of unlimited and curvature-rate limited responses. ——— $k_{\theta'} = 4$, $k_y = 1$, $k_l = 1$, $V = 0.2$ m/s (no limiting); – – – $k_{\theta'} = 10$, $k_y = 1.038$, $k_l = 0.1$, $V = 0.2$ m/s; (b) Curvature, κ, against time. $k_{\theta'} = 10$, $k_y = 1$, $k_1 = 0.1$, $V = 0.2$ m/s.

simulated comparison of a curvature-rate-limited system, with the above selection of parameters, and the original unlimited control system. Although the two systems have similar rise times, the form curvature takes in the curvature-rate-limited system is much smoother. Fig 11b shows the curvature of the vehicle during test and indicates that the vehicle turned right (positive curvature) and then left (negative curvature), gradually, as it approached its new demand path. The crosses on this figure indicate the curvature at specific control interrupts and can be compared with those of the original system in Fig 5d, where there is an initial large change in curvature between two consecutive control interrupts followed by a series of much smaller changes. Fig 11 indicates that, rather than having a large step change in curvature immediately after a step disturbance, the limiting block spreads changes in curvature much more evenly over the whole of the steering process, thus reducing the peak torque demand on the stepper motors for a given rise time.

8. Conclusion

In this paper, the formulation, analysis and the subsequent modification of a steering-control system for an experimental autonomous vehicle has been described. The success of the controller is largely due to the formulation of a good control rule, which states that a local demand heading pointing towards the vehicle's current demand path should be generated in proportion to the local perpendicular distance error. Using this demand heading, a demand turning curvature proportional to the difference between the vehicle's local heading and the local demand heading is generated. Although this control rule is very simple, it has proved successful, largely because it establishes a link between the vehicle's two degrees of freedom y and θ' relative to its demand path.

It has been shown how the motion of the vehicle can be described by a pair of first-order differential equations and the control analysed in a state space format. This analysis generates equations relating the control constants to second-order criteria such as the damping factor and rise time of the system.

Results have shown that although the system performs well when the experimental AGV is asked to follow a line, demand path curvature, which is zero for a straight line, needs to be treated as an input to the control system in order to obtain a compatible performance in curve tracking.

In order to keep the control system performance independent of velocity, the controller parameters should be chosen in inverse proportion to velocity. This generates sensible behaviour whereby the vehicle turns more steeply towards its demand path when it is travelling slowly, thus permitting the vehicle to reach its goal position with greater accuracy.

A modification to the control system includes a method of curvature-rate limiting that prevents stalling of the stepper motors when the vehicle is subjected to a large position correction, and yet behaves in a linear and therefore predictable manner. With such curvature-rate limiting included in the control system, it has been shown how the control parameters can be tuned to give a system performance that is similar to the original system without curvature rate limiting, but has the added advantage of placing smaller demands on the stepper-motor drives.

Although some of the control aspects described in this paper, such as curvature rate limiting, are specific to the independent stepper-drive steering mechanism, the initial analysis of the basic control rule may be applied to other steering mechanism. In such cases, the specific transfer function of the steering mechanism (and possibly some form of compensation) would replace that of the curvature-rate-limit block, and the system would be reassessed in order to choose parameters that give critical damping and the best rise time that is possible for that specific steering mechanism.

9. Acknowledgements

The authors gratefully acknowledge the financial support received from ICI PLC in support of this work. The helpful guidance and advice received from Mr M. Gladders of ICI PLC is also gratefully acknowledged.

10. References

Anon. 1985a. 'Rugged AGV takes three tonne load', *Materials Handling News*, Feb.

Anon. 1985b. 'Computer Manufacturer meets Automation Book with Material Handling', *Materials Handling Engineering*, July.

Brooks, R. A. 1986. 'A Robust Layered Control System for a Mobile Robot', *IEEE J Robotics and Automation*, **RA-2**, (1), 14–23.

Cormier, W. H. and Fenton, R. E. 1980. 'On the Steering of Automated Vehicles – A Velocity-Adaptive Controller', *IEEE Trans on Vehicular Tech*, **VT-29**, (4), 375–385.

Crowley, J. L. 1985. 'Navigation for an Intelligent Mobile Robot', *IEEE J Robotics and Automation*, **RA-1**, (1), 31–41.

Durrant-Whyte, H. F. 1987. *Integration, coordination and control of multi-sensor robot systems*. Kluwer Academic Press, USA.

Elfes, A. E. 1986. 'A Sonar Based Mapping and Navigation System', *Proc IEEE Conf on Robotics and Automation*, San Francisco, USA, 249–265.

Elfes, A. E. and Tulukdar, S. N. 1983. 'A Distributed Control System for the CMU Rover', *Proc 1983 IJCAI*, 830–833.

Fenton, R. E., Melocik, G. C. and Olson, K. W. 1976. 'On the Steering of Automated Vehicles: Theory and Experiment', *IEEE Trans on Autom Cont*, **AC-21**, (3), 306–315

Giralt, G., Sobek, R. and Chatila, R. 1979. 'A Multi-Level Planning and Navigation System for a Mobile Robot: A First Approach to Hilare', *Proc Int Symp of Robotics Res*, Tokyo, Japan, 335–338.

Harmon, S. Y. 1987. 'The Ground Surveillance Robot (GSR): An Autonomous Vehicle Designed to Transit Unknown Terrain', *IEEE J of Robotics and Automation*, **RA-3**, (3) 266–279.

Hongo, T., Arakawa, H., Sugimoto, G., Tange, K. and Yamamoto, Y. 1987. 'An Automatic Guidance System of a Self-Controlled Vehicle', *IEEE Trans on Ind Electron*, **IE-34**, (1), 5–10.

Kande, T., Thorpe, G. and Whittaker, W. 1986. 'Autonomous Land Vehicle Project at CMU', *Proc 1986 Computer Conf*, Cincinnatti, USA, 71–80.

Kim, O. H. 1987. 'Optimal Steering Control of an Auto-Guided Vehicle with Two Motored Wheels', *Trans IMC*, **9**, (2), 58–63.

Komoriya, K., Tachi, S. and Tanie, K. 1986. 'A Method of Autonomous Locomotion for Mobile Robots', *Advanced Robotics*, **1**, (1), 3–19.

Krough, B.H. 1984. 'A Generalised Potential Field Approach to Obstacle Avoidance Control', *Robotics Research Conference Papers*, Robotics International of SME, Dearborn, MI, USA.

Nilsson, N. J. 1969. 'A Mobile Automation: An Application of Artificial Intelligence Techniques', *Proc 1st IJCAI*, 509–520.

Pears, N. E. 1989. *The Low-level Guidance of an Experimental Autonomous Vehicle*, PhD Thesis, University of Durham.

Pears, N. E. and Bumby, J. R. 1990. 'Guidance of an Autonomous Guided Vehicle Using Low Level Ultrasonic and Odometry Sensor Systems' *Trans IMC*, **1**, (5).

Steer, B. 1985. *Navigation for the Guidance of a Mobile Robot*, PhD Thesis, 75–98.

Stephens, P, Robins, M. and Roberts, M. 1983. 'Truck Location Using Retroflective Strips and Triangulation with Laser Equipment' *Proc 2nd European Conf on Automated Manufacture*, Birmingham, 271–282.

Warwick, K. and Brady, J. M. 1986. *A bibliography for autonomous guided vehicle research*. Report No. OVEL 1631/86, University of Oxford.